ACS OMEGA

http://pubs.acs.org/journal/acsodf

Article

Experimental Study on Microwave-Assisted Ignition and Combustion Characteristics of ADN-Based Liquid Propellant

Yangyang Hou, Yusong Yu,* Xuhui Liu, Jun Chen, and Tao Zhang

Cite This: *ACS Omega* 2021, 6, 22937–22944

Read Online

ABSTRACT: Microwave-assisted ignition is a new ignition method, which has the advantages of reliable ignition and high ignition energy and requires no preheating. In this study, experimental methods were used to study the microwave-assisted ignition and combustion characteristics of ADN-based liquid propellant, and the effects of microwave power and propellant flow rate on combustion flame structure, spectral emission characteristics, and flame temperature were investigated. In the experiment, a microwave-assisted ignition experimental device was established first. The ADN-based liquid propellant was injected into the microwave high-energy region from the bottom of the resonator through a hollow straight tube with an inner diameter of 1 mm, and the gas was introduced in a coaxial manner. The research results demonstrated that when the microwave power increased from 1000 to 2000 W, the flame height increased from 11.12 to 17.32 mm; the free radical intensity of C_2*, NH_2, and HNO* increased significantly; the flame temperature increased by about 28.9%. The increase in microwave power is helpful to the generation of intermediate products and the combustion performance of propellant is better. When the propellant flow rate was increased from 25 to 45 mL/min, it was found that the spray combustion effect was the best when the propellant flow rate was 30 mL/min, the flame height increased by 25.2%, and the flame temperature increased by about 11.3%.

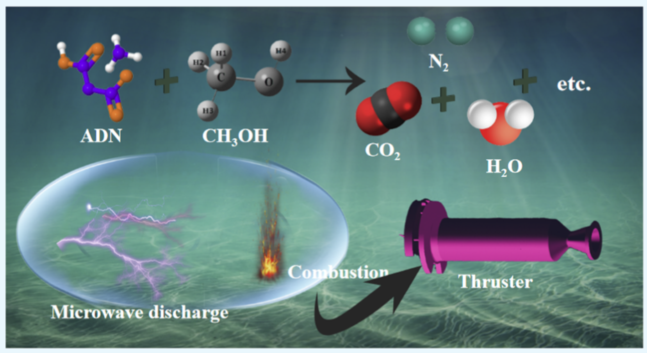

1. INTRODUCTION

With the rapid development of aerospace technology, problems related to environmental protection and sustainable use of traditional propellants have become increasingly prominent. To this end, the development of pollution-free, recyclable, and green propellants has important scientific significance and application value. Ammonium diamide (ADN)-based liquid propellant is a new type of high-performance, low-toxicity green monopropellant, which, in recent years, has received extensive attention in the military and aerospace fields, representing a new research direction and development trend of space propulsion technology with good application prospects.[1]

ADN-based liquid thrusters, which are currently used on satellites, mostly use the catalytic decomposition method to ignite the ADN-based liquid propellant.[2−4] Some scholars also try to use the emerging thermal ignition.[1,5] The limitations related to the ignition method hinder the development of the green ADN-based propellants in the aerospace field; thus, it is urgent to find a reliable and stable ignition method. In recent years, plasma-assisted ignition has developed rapidly as a new combustion technology in the aeroengine field, and its main principle is to promote auxiliary fuel ignition through plasma discharge.[6−11] Common plasma discharges include filamentary discharge,[12] corona discharge,[13] streamer discharge,[14] microwave discharge,[15] surface discharge,[16] and nanosecond pulsed repetitive discharge.[17] Bulat et al. investigated a subcritical microwave streamer discharge to ignite air−fuel mixtures and proved that microwave streamer ignition combustion has a faster combustion speed and a higher combustion efficiency compared to spark combustion.[18] The microwave-assisted ignition technology mainly uses the microwave discharge principle to ignite ADN-based liquid propellant.

According to the existing literature in the field of automobile engines, microwave-assisted ignition technology has been relatively mature, and good test results have been reported.[19−21] Hwang et al. investigated the effect of microwave-assisted plasma ignition on the development of laminar flame in a constant volume combustion chamber (CVCC) and revealed that compared to traditional spark

Received: July 8, 2021
Accepted: August 16, 2021
Published: August 26, 2021

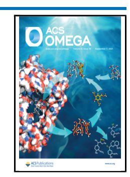

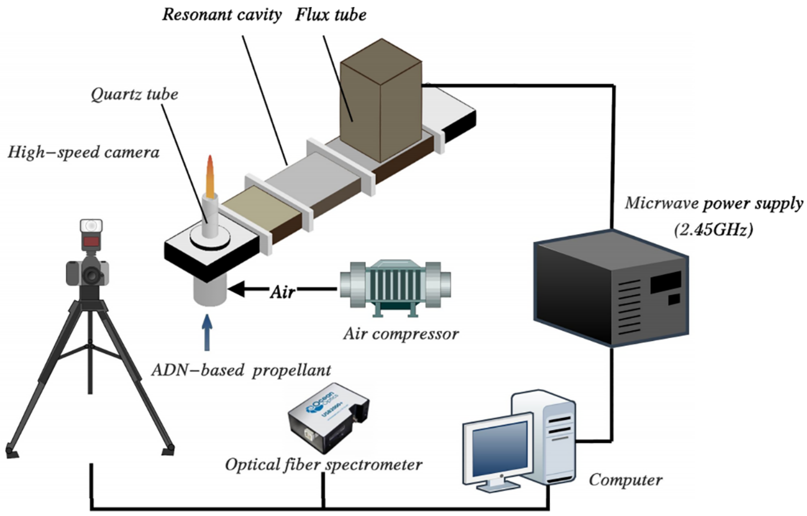

Figure 1. Schematic diagram of the experimental setup.

ignition, microwave plasma ignition has an apparent lean limit.[22] More specifically, the flame expansion time increased significantly, and the flame speed increased up to 20%. Consequently, the possibility of applying the microwave ignition technology in propulsion systems has been raised; however, currently there are only a few studies on the microwave ignition characteristics of ADN-based liquid propellants.

In this research, the possibility of microwave-assisted ignition and combustion of an ADN-based liquid propellant in the discharge cavity is experimentally investigated. Through the coupling mechanism of microwave plasma in the electromagnetic field, the air plasma is first ignited to promote the combustion of the ADN-based liquid propellant and the effects of microwave power and propellant flow rate on the combustion flame characteristics are studied. In the combustion process of ADN-based liquid propellants, several branched reaction processes take place and a variety of intermediate free radicals are produced. Based on the band spectra emitted by flames, in this work, a preliminary study on the flame spectrum at the initial stage of ADN-based liquid propellant combustion is conducted for the first time.

2. EXPERIMENTAL DESIGN AND METHODS

2.1. Experimental Setup. A schematic diagram of the experimental setup is illustrated in Figure 1. The experimental system used in this study comprised a microwave plasma generation system, a propellant supply system, an intake and exhaust system, and a spectrum test system. The microwave plasma generation system consisted of a microwave power supply, magnetron, tuner, and waveguide components. The microwave power supply could provide 2.45 GHz microwave radiation, and the maximum power of the magnetron was 3 kW. In the experiments, an Ocean USB 2000+ fiber optic spectrometer was employed to collect the flame emission spectrum information. The spectrum test system consisted of a light probe, an optical fiber wire, a fiber optic spectrometer, and a computer control unit. The optical fiber spectrometer had a maximum measurement range of 200−900 nm, a resolution of 1.5 nm, and a detection integration time of 1 ms. To ensure that the measured signal comes from the target object, a collimating lens was added to the optical fiber probe to make the radiation signal of the target object enter the probe in the form of parallel light.

The experiments were mainly performed in an atmospheric environment, using air as the discharge medium. Before switching on the microwave generator, a steady airflow was first ensured in the discharge chamber. The airflow rate is precisely controlled through a 2 MPa high-pressure air source by adjusting the needle valve and monitoring the airflow meter. After the plasma was excited, the ADN-based propellant spray was injected into the discharge cavity. The ADN-based propellant is precisely controlled by a peristaltic pump and is injected into the discharge region of the resonant cavity through a circular tube with a 1 mm inner diameter. The air plasma was used to ignite the propellant; finally, a jet flame was generated and stable combustion was established.

2.2. Microwave Discharge. Microwaves of a specific frequency were used to resonate in the resonant cavity and form a strong electromagnetic field. The high-frequency electrons can gain enough energy by colliding with the surrounding particles to excite atoms and molecules to emit light, which is known as microwave discharge. The motion direction of the electrons changes constantly through continuous elastic collisions; thus, they gradually gain enough energy from the microwave field to excite and ionize atoms and molecules. There is no definite electrode for microwave discharge, mainly capacitive coupling discharge, with a frequency of 300 MHz to 300 GHz and a typical operating frequency of 2.45 GHz. Due to the Lorentz force exerted on the moving electrons, which is generated by the magnetic field in the discharge chamber, the electrons gain a certain amount of energy, and the high-energy electrons ionize the surrounding gas to form plasma.

3. RESULTS AND DISCUSSION

3.1. Effect of Microwave Power on Combustion Characteristics. The incident microwave power reflects the intensity of the energy fed into the microwave and is one of the key factors affecting the gas breakdown discharge. Figure 2 demonstrates the jet flame state in the quartz tube at different time points under atmospheric pressure when the microwave power values were 1000, 1250, 1500, 1750, and 2000 W. It is known that the randomness of the plasma jet direction depends mainly on the electron density distribution, which can

https://doi.org/10.1021/acsomega.1c03591
ACS Omega 2021, 6, 22937−22944

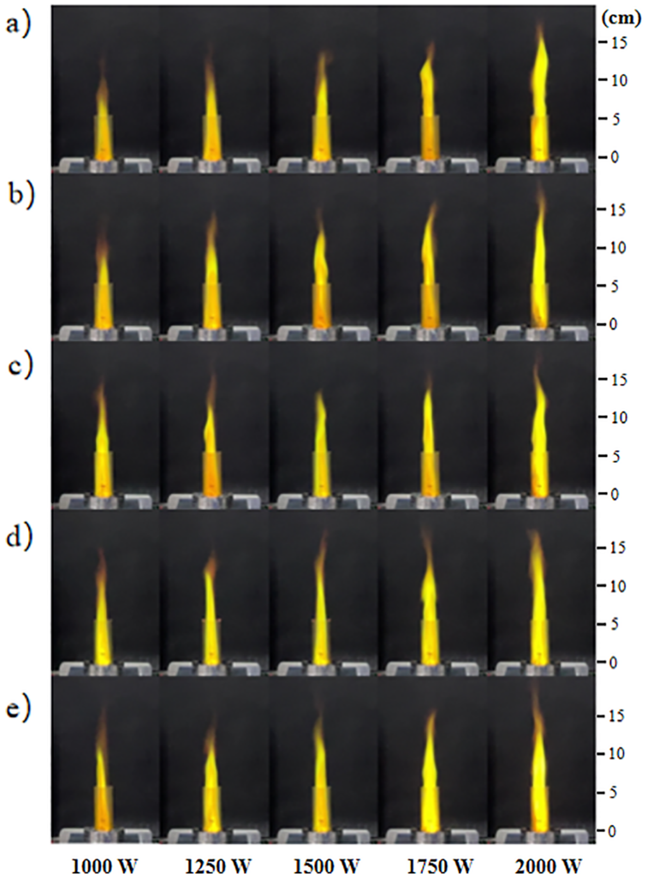

Figure 2. Jet flame images under different microwave powers at (a) t = 5 s, (b) t = 10 s, (c) t = 15 s, (d) t = 20 s, and (e) t = 25 s after ignition.

be controlled by the position of the discharge channel. To compare the effects of different microwave power on the jet flame, it was necessary to ensure that, during the experiments, the plasma jet was always in the same direction. To this end, the position of the tungsten needle in the discharge cavity remained unchanged, ensuring that, after the gas breakdown, the electron concentration was uniformly distributed.

In general, microwave-assisted ignition provides a directional driving force for the front end of the plasma jet flame and accelerates its directional development. The jet flame extends outward into the quartz tube at the upper end of the discharge chamber. Based on the comparison photographs in Figure 2, the following observations can be made: (1) When the microwave ignites the air plasma, a bright and strong light is emitted in the discharge cavity. After the ADN-based liquid propellant is injected, the jet flame gradually stabilizes and exhibits a characteristic yellow-green flame. (2) When the microwave power is low, the electric field can ionize only a small amount of air into the plasma at the nozzle tip; thus, the plasma torch length is short. When the microwave power increases, the flame height increases with the increasing discharge intensity. (3) When the jet flame is stable, the flame shape at different time points has certain differences, while the flame height is practically the same. This is attributed to the fact that, while the upward disturbance of the air induces a small range of fluctuations to the jet flame, the microwave power is constant, the electric field intensity does not change, and thus, the changes in the flame height are almost negligible.

In addition, some white particles were observed on the quartz tube. This is due to the fact that the ADN-based liquid propellant was not completely burned in the discharge chamber, and the residual propellant was driven upward by the air and ejected out of the quartz tube along with the jet. It is worth noting that when the microwave power is low, the microwave energy coupled into the discharge cavity is not sufficient to completely ionize the air therein. The energy in the discharge cavity increases with increasing microwave power until the working gas has been completely broken down. The discharge fills the lower end of the quartz tube and, as the gas flow diffuses, extends to the outside of the quartz tube.

The average height of the ADN-based liquid propellant jet flame under different microwave power levels is plotted in Figure 3, and the estimated maximum error in the jet height is

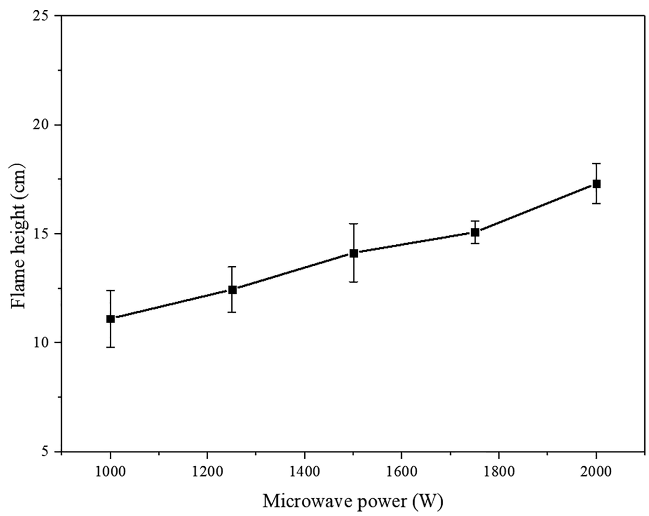

Figure 3. Average flame height of the ADN-based liquid propellant under different microwave power levels in an atmospheric environment; the error bars represent the approximate value.

about 2 pixels. It can be observed that the jet flame heights under the different microwave power levels were 11.12, 12.46, 14.14, 15.08, and 17.32 mm. When the microwave power increased from 1000 to 2000 W, the maximum increase in the plasma jet flame height was about 55.8%. This is because when the microwave power is low, the electric field intensity in the discharge cavity is low as well, and only a small amount of the air in the cavity can be ionized into plasma. At this point, the introduced propellant cannot be completely burned; thus, the jet flame is relatively small. With the increase of power, the initial discharge field of the tip conductor has a stronger resonance, which increases the electron transition rate near the discharge tip. During this process, the electrons gain higher energy from the stronger electric field for collision and excitation. The concentration of discharge particles near the discharge tip increases; as a result, the height of the plasma jet increases accordingly.

Free radicals in flames can be mainly excited in two ways: thermal or chemical excitation.[23] During the combustion of the ADN-based liquid propellant, a large number of free radicals are generated, which include important intermediate products, such as N_2O, NO, NH_2, NH_3, CO_2, and H_2O. Gaydon compiled the emission spectra of some free radicals.[24] As shown in Table 1, where it can be observed that NH_2* is mainly distributed in the visible-light region and its radiation

https://doi.org/10.1021/acsomega.1c03591
ACS Omega 2021, 6, 22937−22944

Table 1. Wave Bands of the Radicals in the Flame of ADN-Based Liquid Propellant

radical	wavelength (nm)
CO_2	400−543
NH_2	526.5−665.2
CH*	304.6
Na*	588.6
K*	766.4
HNO*	763.3−766.6, 793−797.2
C_2*	469−473, 510−516

wavelength is usually 544 nm, while that of CO_2 is 543 nm. In addition, the emission spectra of Na* and K* were detected in the flame. A large number of studies have reported that the air contains alkali metal salts, the sources of which in the flame generally include (1) the salt in oxygen; (2) the salt adsorbed on the surface of experimental equipment; and (3) the salt in sweat that enters into the flame with the airflow. Experiments have demonstrated that there are no apparent band peaks in the ultraviolet region of 200−380 nm, where the spectral intensity is weak, and obvious radical peaks appear in the visible-light and near-infrared regions at 380−780 and 780−1100 nm, respectively. Figure 4 illustrates the spectra of the flame under different microwave power levels collected and processed by a fiber optic spectrometer. In addition, measurements are usually averaged over 10 s for each spectral calibration to reduce the effect of measurement errors. In these spectra, characteristic bands of CH*, HNO*, NO_2*, Na*, and K* can be observed. The focus of the present work is the observation of these free radical emitters during the combustion of ADN-based liquid propellant. It can be clearly seen that changing the microwave power level has no significant effect on the wavelength range corresponding to the free radical emission peaks in the spectrum, while it has a certain effect on the signal intensity of the free radicals.

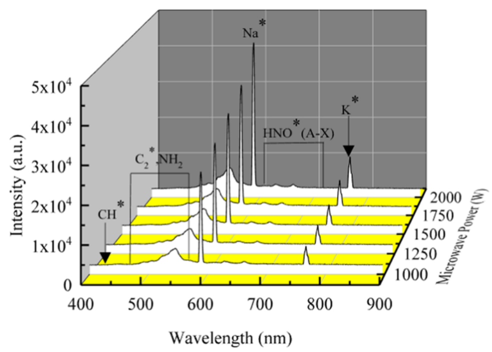

Figure 4. Corrected emission spectral distribution of the ADN-based liquid propellant jet flame under different microwave power levels.

Figure 5a presents the emission spectrum characteristics of the C_2* and NH_2 radicals in detail. In the initial flame of the ADN-based liquid propellant combustion, the emission spectra of the C_2* radicals were mainly the Swan and Philips bands. Characteristic peaks were observed at 512.9, 516.5, and 547 nm and at 771.5 and 810.8 nm in the infrared band; although the spectral intensity was high, the characteristics were not apparent. The generation of C_2* free radicals concerns two mechanisms: one is the direct reaction of groups containing multiple carbon atoms with other groups; the other is that saturated hydrocarbon molecules undergo a dehydrogenation reaction; then, multiple unsaturated C-containing groups are formed, which assemble a carbon chain. Due to the instability of the structure, the carbon chain separates any excess carbon atoms, forming relatively stable C_2* radicals. The NH_2* band appears strong in oxygen/ammonia and hydrogen/nitrous oxide flames; however, it is not that intense in other flames containing hydrogen and nitrogen. Figure 5b exhibits the spectral band of the HNO* radicals. In general, the bands in the region of 650−900 nm are attributed to HNO* emission.[25] It has been found that the radiation intensity of the C_2*, NH_2, and HNO* free radicals increased gradually with the increasing microwave power. In addition, the radiation intensity of the free radicals increased exponentially with the increasing power. This is because, as the microwave power increases, the combustion reaction of the ADN-based liquid propellant becomes more violent, and the concentration of the free

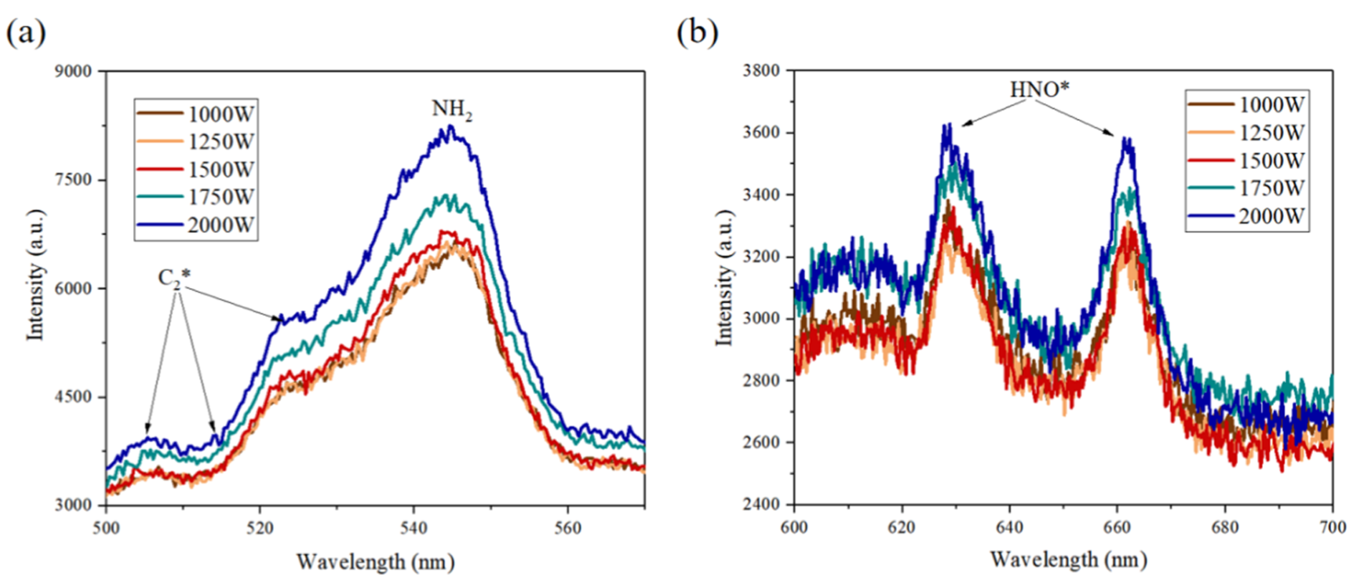

Figure 5. (a) C_2*, NH_2 emission bands of the ADN-based liquid propellant jet flame under different microwave power levels. (b) HNO* emission bands of the ADN-based liquid propellant jet flame under different microwave power levels.

https://doi.org/10.1021/acsomega.1c03591
ACS Omega 2021, 6, 22937−22944

radicals generated during the combustion reaction increases as well. This is macroscopically manifested as an increase in the radiation intensity of free radicals, such as C_2*, NH_2, and HNO*.

3.2. Effect of Propellant Flow Rates on Combustion Characteristics.

Figure 6 demonstrates the flame height variation of the propellant jet under different flow rates. In all cases, the microwave power was constant at 1500 W. When the propellant flow rate was 25−45 mL/min, it can be observed that the jet height increased first, then decreased, and finally increased. The overall range of the flame height change was small. This is due to the fact that the increase in the propellant flow rate corresponds to an increase in the number of propellant droplets in the discharge chamber, and the combustion of the flame is mainly affected by the atomization performance of the propellant. When the flow rate is 30 mL/min, the atomization of the ADN-based liquid propellant in the discharge cavity is better and the combustion is more complete. When the flow rate continues to increase, the jet height increases as well. Nevertheless, due to the high jet flow rate, some propellant droplets are not completely burnt but ejected out of the tube along with the airflow. It is worth noting that the atomization of the propellant in the discharge cavity is affected by several factors. The spray and droplet dynamics are research hotspots. The turbulence−spray−combustion interaction mechanism is also under discussion. Consequently, a spray combustion mechanism in the discharge cavity caused by microwave-assisted ignition has an important scientific research value.

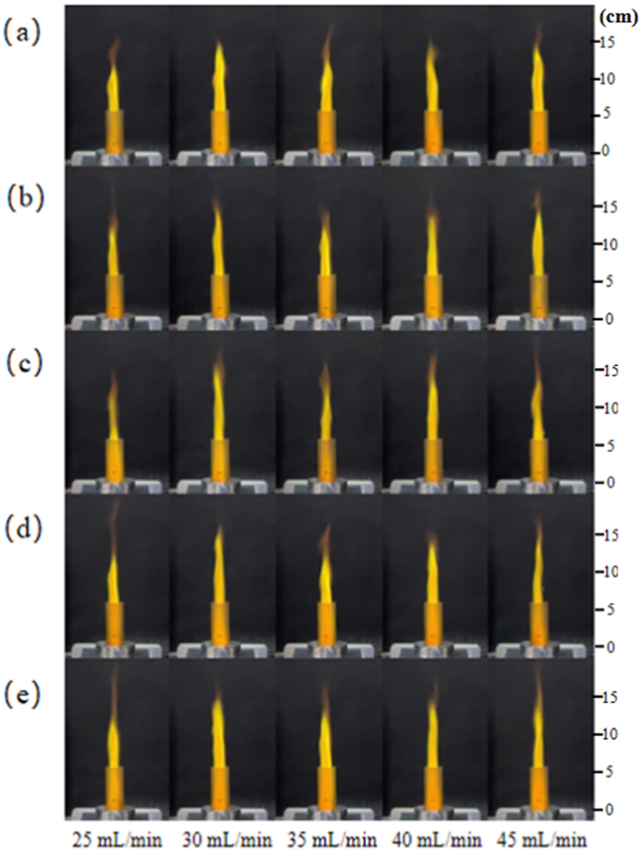

Figure 6. Jet flame images under different propellant flow rates at (a) t = 5 s, (b) t = 10 s, (c) t = 15 s, (d) t = 20 s, and (e) t = 25 s after ignition.

Figure 7 plots the average height of the ADN-based liquid propellant jet flame under different propellant flow rates. At different tested flow rates, the height of the jet flame was found to be 13.32, 16.76, 14.18, 15.26, and 15.87 mm, respectively. It can be observed that when the propellant flow rate ranged between 25 and 45 mL/min, the maximum height difference was about 25.8%. Unlike the effect of the microwave power on the jet flame height, discussed in Section 3.1, the effect of the propellant flow rate on the flame height did not exhibit a regular trend, and the flame height did not change significantly. The experimental results revealed that, under a high flow rate, the jet flame height increased significantly; however, the flame shape became more slender, and there were a lot of propellant crystal residues within the discharge chamber and the lower half of the quartz tube. This is due to the fact that when the nozzle diameter is fixed (0.1 mm), the higher propellant flow rate is difficult to ensure a good atomization effect, the propellant particles cannot achieve a large-area contact with the air plasma jet flame, and the combustion reaction in the discharge cavity is difficult to proceed.

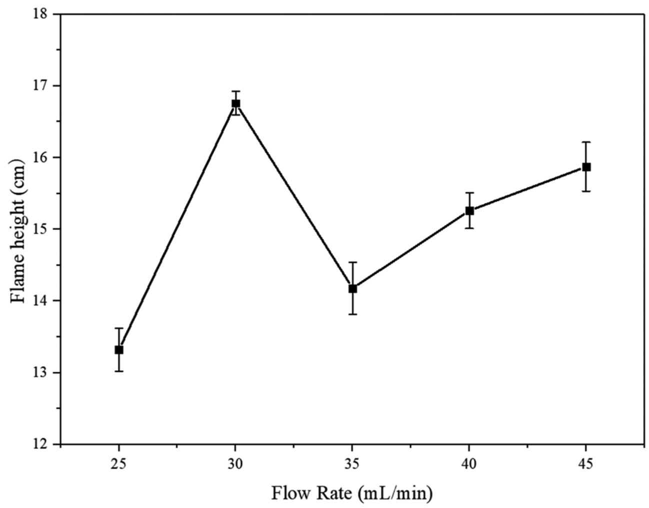

Figure 7. Average flame height of the ADN-based liquid propellant under different propellant flow rates in an atmospheric environment; the error bars represent the approximate value.

Figure 8 exhibits the spectra of the ADN-based liquid propellant jet flame under the five tested propellant flow rates with spectral assignments for the most intense bands. Theoretically, in the combustion of nitrogen-containing hydrocarbon fuels, a variety of ground- and excited-state radical radiation lines can be found in the combustion flame, which includes OH*, CH*, C_2*, HCN, NH_2, CO_2, and HNO*, as well as other free radicals and alkali metals, such as Na* and K*. Consistent with the spectra obtained under different microwave power levels, the propellant flow rate was found to have no significant effect on the wavelength range corresponding to the free radical emission peaks, while the free radical radiation intensity corresponding to different propellant flow rates was different. In particular, CH* radicals are generated in the first sharp temperature rise area of the flame reaction zone; these radicals have a short life and low-concentration chemiluminescence characteristics and are mainly distributed in the visible-light band. The main reaction

https://doi.org/10.1021/acsomega.1c03591
ACS Omega 2021, 6, 22937−22944

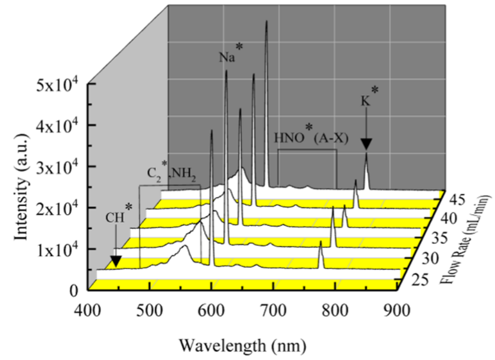

Figure 8. Corrected emission spectral distribution of the ADN-based liquid propellant jet flame obtained under different propellant flow rates.

paths are $C_2 + OH{=}CH^* + CO$ or $C_2H + O{=}CH^* + CO$. Moreover, HNO* appeared also in the very early stage of the reaction, with the main reaction paths being $HCO + NO{=}HNO + CO$, $CH_3 + NO_2{=}HNO + CH_2O$, and $CH_3O + NO{=}HNO + CH_2O$.

Figure 9 presents the emission spectrum characteristics of the C_2*, NH_2, and HNO* radicals under different propellant flow rates. It can be observed that the flow rate of the ADN-based liquid propellant has a great impact on jet flame. As mentioned above, when the flow rate is high, the flame height increases abnormally and the flame becomes slenderer. For the two identified emitters (C_2*, NH_2), the intensity of free radical emission versus the propellant flow rate is presented in Figure 9a, where several trends can be observed. First, each contour displays a maximum value. For the C_2* and NH_2 free radicals, the maximum radiation intensity increases first, then decreases, and continues to increase with the increasing propellant flow. Figure 9b shows that some profiles exhibit more than one local maxima, especially those of HNO*. In addition, the wave-packet generated between 540 and 550 nm may be the result of the combination of multiple species; possible combinations include NH_2 and CO_2 or a mixture of nitrogen-containing substances. All species presented emissions due to flame enveloping below the surface. Due to the limitations of the experimental device, the spectral emission characteristics of several intermediate products in the combustion reaction, such as OH*, N_2O, and H_2O, are not observed.

3.3. Flame Temperature of Microwave-Assisted Ignition.

Temperature is one of the most important physical parameters of flames, and the characterization of flame temperature is of great significance in understanding the flame combustion process. The maximum error in temperature measurements by thermocouples is ∼4%. In Figure 10, the ADN-based liquid propellant jet flame temperature under the microwave-assisted ignition mode is presented as a function of microwave power and propellant flow rate. The result shows that the microwave power and propellant flow rate have varying degrees of influence on the flame temperature. The effect of microwave power on the temperature is mainly

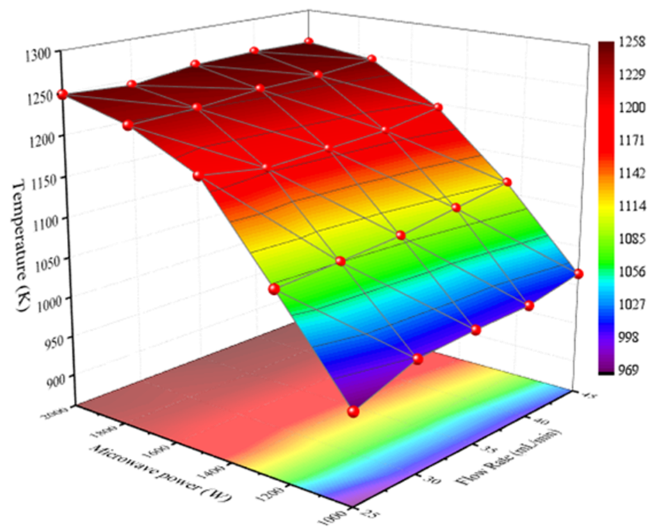

Figure 10. Temperature diagram of the ADN-based liquid propellant jet flame as a function of microwave power and flow rate in an atmospheric environment.

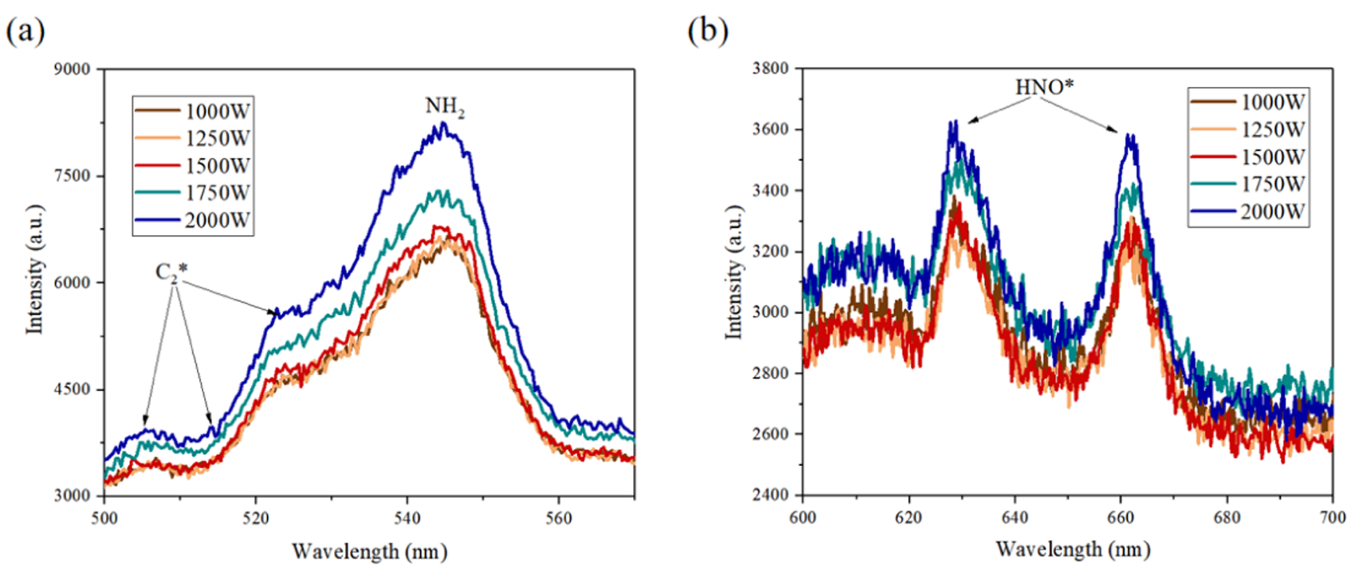

Figure 9. (a) C_2* and NH_2 emission bands of the ADN-based liquid propellant jet flame under different propellant flow rates. (b) HNO* emission bands of the ADN-based liquid propellant jet flame under different propellant flow rates.

attributed to the fact that the higher the energy fed by the microwave, the more violent the discharge and gradually more clear the flame contour, which are more conducive to the combustion and decomposition of the ADN-based liquid propellant. Since the ADN-based liquid propellant is a high-energy material, when the amount of energy fed by the microwave is small, the combustion promotion effect of the propellant is not significant. When the microwave power is above 1500 W, a qualitative leap in the flame temperature can be observed. Nevertheless, since the propellant flow rate has no apparent effect on atomization, its effect on temperature is small.

4. CONCLUSIONS

The ADN-based liquid propellant can be successfully ignited through microwave-assisted ignition. Compared to traditional catalytic combustion, it has better ignition performance and can achieve multipoint ignition in space, which has a good application prospect. The conclusions of the present study are summarized as follows:

(1) Under atmospheric pressure, the combustion performance of the ADN-based liquid propellant can be improved to a certain extent with increasing microwave power, and the combustion reaction in the discharge cavity can be more complete. In addition, during the combustion and decomposition processes of the ADN-based liquid propellant, the intensity of NH_2, HNO*, and other free radicals was also significantly increased. This means that a higher microwave power level may be more conducive to the combustion reaction of the ADN-based liquid propellant in the discharge cavity.

(2) Under a constant microwave power level, the flow rate of the ADN-based liquid propellant injected into the discharge cavity was changed, and according to the results, the flame combustion characteristics did not exhibit a regular change trend. It was found that when the flow rate is 30 mL/min, the ADN-based liquid propellant has a good atomization effect in the discharge chamber, and the fuel can come into full contact with the air plasma flame and burn, maintaining a stable jet flame shape.

(3) According to the experimental results, after the ADN-based liquid propellant has been successfully ignited, stable and continuous combustion can be achieved, and sufficient energy can be produced to ensure the operation of the ADN-based thruster. Under atmospheric conditions, microwave-assisted ADN-based liquid propellant ignition is feasible; it can be used to replace the traditional catalytic combustion technology and has a potential application in the aerospace field.

AUTHOR INFORMATION

Corresponding Author

Yusong Yu − *Department of Power and Energy Engineering, Beijing Jiaotong University, Beijing 100044, China*; Email: yusong_yu@163.com

Authors

Yangyang Hou − *Department of Power and Energy Engineering, Beijing Jiaotong University, Beijing 100044, China*; orcid.org/0000-0001-7547-2553

Xuhui Liu − *Beijing Insititute of Control Engineering, Beijing 100190, China*

Jun Chen − *Beijing Insititute of Control Engineering, Beijing 100190, China*

Tao Zhang − *Beijing Insititute of Control Engineering, Beijing 100190, China*

Complete contact information is available at: https://pubs.acs.org/10.1021/acsomega.1c03591

Notes

The authors declare no competing financial interest.

ACKNOWLEDGMENTS

The research was supported by the Advanced Space Propulsion Laboratory of BICE and the Beijing Engineering Research Center of Efficient and Green Aerospace Propulsion Technology (LabASP-2020-08).

REFERENCES

(1) Li, H.-M.; Li, G.-X.; Li, L.; Yao, Z.-P. Experimental study on thermal ignition and combustion of droplet of ammonium dinitramide based liquid propellant in different oxidizing gas atmospheres. *Acta Astronaut.* **2020**, *169*, 40−49.

(2) Amrousse, R.; Hori, K.; Fetimi, W.; Farhat, K. HAN and ADN as liquid ionic monopropellants: Thermal and catalytic decomposition processes. *Appl. Catal., B* **2012**, *127*, 121−128.

(3) Shmakov, A. G.; Bol'Shova, O.; et al. Thermal decomposition of ammonium dinitramide vapor in a two-temperature flow reactor. *Combust., Explos. Shock Waves* **2002**, *38*, 284−294.

(4) Wingborg, N.; Larsson, A.; Elfsberg, M.; Appelgren, P. In *Characterization and Ignition of ADN-Based Liquid Monopropellants*, 41st AIAA/ASME/SAE/ASEE Joint Propulsion Conference & Exhibit, Tucson, 2005; p 4468.

(5) Wilhelm, M.; Negri, M.; Ciezki, H.; Schlechtriem, S. Preliminary tests on thermal ignition of ADN-based liquid monopropellants. *Acta Astronaut.* **2019**, *158*, 388−396.

(6) Ju, Y.; Sun, W. Plasma assisted combustion: Dynamics and chemistry. *Prog. Energy Combust. Sci.* **2015**, *48*, 21−83.

(7) Gan, Y.; Tong, Y.; Ju, Y.; Zhang, X.; Li, H.; Chen, X. Experimental study on electro-spraying and combustion characteristics in meso-scale combustors. *Energy Convers. Manage.* **2017**, *131*, 10−17.

(8) Wang, X.; Gao, Y.; Zhang, S.; Sun, H.; Li, J.; Shao, T. Nanosecond pulsed plasma assisted dry reforming of CH_4: the effect of plasma operating parameters. *Appl. Energy* **2019**, *243*, 132−144.

(9) Kim, W.; Godfrey Mungal, M.; Cappelli, M. A. The role of in situ reforming in plasma enhanced ultra lean premixed methane/air flames. *Combust. Flame* **2010**, *157*, 374−383.

(10) Kai, Z.; Song, F.; Jin, D.; Xu, S.; Huang, S.; et al. Experimental investigation on the cracking of pre-combustion cracking gas with gliding arc discharge plasma. *Int. J. Hydrogen Energy* **2021**, *46*, 9019−9029.

(11) Sun, H.; Zhang, S.; Gao, Y.; Huang, B.; Zhang, C.; Shao, T. Non-oxidative methane conversion in diffuse, filamentary, and spark regimes of nanosecond repetitively pulsed discharge with negative polarity. *Plasma Processes Polym.* **2019**, *16*, No. 1900050.

(12) Bogaerts, A.; Zhang, Q.-Z.; Zhang, Y.-R.; Van Laer, K.; Wang, W. Burning questions of plasma catalysis: Answers by modeling. *Catal. Today* **2019**, *337*, 3−14.

(13) Kang, M. S.; Yu, G.; Shin, J.; Hwang, J. Collection and decomposition of oil mist via corona discharge and surface dielectric barrier discharge. *J. Hazard. Mater.* **2021**, *411*, No. 125038.

(14) Filimonova, E. A.; Dobrovolskaya, A. S.; Bocharov, A. N.; Bityurin, V. A.; Naidis, G. V. Formation of combustion wave in lean propane-air mixture with a non-uniform chemical reactivity initiated by nanosecond streamer discharges in the HCCI engine. *Combust. Flame* **2020**, *215*, 401−416.

(15) Bogdanov, S. A.; Gorbachev, A. M.; Vikharev, A. L.; Radishev, D. B.; Lobaev, M. A. Study of microwave discharge at high power density conditions in diamond chemical vapor deposition reactor by optical emission spectroscopy. *Diamond Relat. Mater.* **2019**, *97*, No. 107407.
(16) Assadi, A. A.; Loganathan, S.; Tri, P. N.; Gharib-Abou Ghaida, S.; Bouzaza, A.; Tuan, A. N.; Wolbert, D. Pilot scale degradation of mono and multi volatile organic compounds by surface discharge plasma/TiO_2 reactor: Investigation of competition and synergism. *J. Hazard. Mater.* **2018**, *357*, 305−313.
(17) Bechane, Y.; Fiorina, B. Numerical investigations of turbulent premixed flame ignition by a series of Nanosecond Repetitively Pulsed discharges. *Proc. Combust. Inst.* **2021**, *38*, 6575−6582.
(18) Bulat, M. P.; Bulat, P. V.; Denissenko, P. V.; Esakov, I. I.; Grachev, L. P.; Volkov, K. N.; Volobuev, I. A. Ignition of lean and stoichiometric air-propane mixture with a subcritical microwave strwamer discharge. *Acta Astronaut.* **2018**, *150*, 153−161.
(19) Zhang, X.; Wang, Z.; Wu, H.; Liu, C.; Cheng, X.; Chen, J.-Y. Propulsive effect of microwave-induced plasma jet on spark ignition of CO_2-diluted CH_4-air mixture. *Combust. Flame* **2021**, *229*, No. 111400.
(20) Le, M. K.; Nishiyama, A.; Serizawa, T.; Ikeda, Y. Applications of a multi-point Microwave Discharge Igniter in a multi-cylinder gasoline engine. *Proc. Combust. Inst.* **2019**, *37*, 5621−5628.
(21) Wang, Z.; Huang, J.; Wang, Q.; Hou, L.; Zhang, G. Experimental study of microwave resonance plasma ignition of methane−air mixture in a constant volume cylinder. *Combust. Flame* **2015**, *162*, 2561−2568.
(22) Hwang, J.; Bae, C.; Park, J.; Choe, W.; Cha, J.; Woo, S. Microwave-assisted plasma ignition in a constant volume combustion chamber. *Combust. Flame* **2016**, *167*, 86−96.
(23) Deleo, M.; Saveliev, A.; Kennedy, L.; Zelepouga, S. OH and CH luminescence in opposed flow methane oxy-flames. *Combust. Flame* **2007**, *149*, 435−447.
(24) Gaydon, A. G. *The Spectroscopy of Flames*, 2nd ed.; Champan and Hall: London, 1974; pp 1−412.
(25) Sheehe, S. L.; Jackson, S. I. Identification of species from visible and near-infrared spectral emission of a nitromethane-air diffusion flame. *J. Mol. Spectrosc.* **2019**, *364*, No. 111185.

https://doi.org/10.1021/acsomega.1c03591
ACS Omega 2021, 6, 22937−22944